Journal of Power Sources 210 (2012) 86–91

Contents lists available at SciVerse ScienceDirect

Journal of Power Sources

journal homepage: www.elsevier.com/locate/jpowsour

A novel sintering method to obtain fully dense gadolinia doped ceria by applying a direct current

Xiaoming Hao, Yajie Liu, Zhenhua Wang*, Jinshuo Qiao, Kening Sun*

School of Chemical Engineering and Environment, Beijing Institute of Technology, Beijing 100081, China

ARTICLE INFO

Article history:
Received 9 January 2012
Received in revised form 1 March 2012
Accepted 2 March 2012
Available online 8 March 2012

Keywords:
Gadolinia doped Ceria
Flash Sintering
Solid Oxide Fuel Cells

ABSTRACT

A fully dense $Ce_{0.8}Gd_{0.2}O_{1.9}$ (gadolinia doped ceria, GDC) is obtained by a novel using a sintering technique for several seconds at 545 °C by applying a direct current (DC) electrical field of 70 V cm^{-1}. The onset applied field value of this phenomenon is 20 V cm^{-1}, and the volume specific power dissipation for the onset of flash sintering is about ~10 mW mm^{-3}. Through contrast with the shrinkage strain of the conventional sintering as well as scanning electron microscopy (SEM) analysis, we conclude that GDC specimens are sintered to fully density under various applied fields. In addition, we demonstrate that the grain size of GDC is decreasing with the increase of applied field and the decrease of sintering temperature. Through calculation, we find that sintering of GDC can be explained by the Joule heating from the applied electrical field.

1. Introduction

Conventional solid oxide fuel cells (SOFCs) with traditional electrolyte yttria-stabilized zirconia (YSZ) operate at the temperature above 800 °C. However, costly materials are required at such a high temperature for other structure components of SOFCs, that is, anode, cathode, interconnectors, and heat exchangers, making the fabrication cost prohibitive which hindering the commercialization of SOFCs [1–3]. Thus lowering the temperature of SOFCs is one main target for recent researchers.

GDC which exhibits four to five times higher ionic conductivity than YSZ at intermediate temperatures (600–700 °C) is a promising electrolyte alternative material [4–9]. Particularly, the micro-SOFC systems [10–13] require high ionic conducting electrolytes at low temperatures in order to be utilized in battery replacement in portable equipment, such as laptops, digital assistants, medical or industrial devices. Despite these advantages, several drawbacks still exist on GDC. One problem is that GDC requires sintering temperature as high as 1350–1600 °C to reach full density [9,14–19]. Such a high temperature will result in large grain size [14–16] which makes it mechanically unstable at the operating conditions of the SOFCs, because of the formation of microstructures with grain sizes in the micron range subsequently offer poor mechanical stability [17–19].

In order to overcome the above difficulties, some processing alternatives had been used. One method was to use nanosized GDC powders as raw materials, much of which were made through co-precipitation, sol–gel, hydrothermal solution and combustion [9,19–25]. Nanosized GDC powders could be sintered to density at lower temperature, but the preparation is too cumbersome to be used extensively. Another method is to use less expensive commercial GDC raw material, and adding sintering aids (Bi_2O_3, Fe_2O_3, Co_2O_3, etc.) to lower the sintering temperature [26–29]. It was reported that GDC could be sintered at temperatures as low as 900 °C with the addition of transition metal oxides (TMO). However this will lower the ionic conductivity of GDC electrolyte at the same time [23,26,30–32]. Sintering aids can lead to an increased grain boundary resistance to ionic conduction [23] likely due to aggregation of the TMO at the grain boundary as a separate phase.

The third method is Spark Plasma Sintering (SPS) technology, also called pulsed electric current sintering (PECS), or field assisted sintering technique (FAST). It is a newly discovered old technique which was traditionally used for compaction and plastic deformation of metallic powders and billets and recently has been used for superfast densification of ceramic powders [33,34]. Spark Plasma Sintering is characterized by simultaneous application of load and pulsed high dc current densities and pressure controlled process. This method has unique advantages for the fabrication of bulk nanocrystalline metals and ceramics [35–38]. Mori [37] reported that the dense sintered Dy-doped CeO_2 bodies with small grain sizes (300 nm) were fabricated using a combined process of SPS and conventional sintering (CS). The micro-domain size in the grain was minimized using the SPS process and the conductivity of the specimens was considerably improved. However, SPS could not make dense Dy-doped CeO_2 sintered bodies over 95% of theoretical calculations. It is because the carbon powders penetrated the sintered

* Corresponding author. Tel.: +86 010 6891 8696; fax: +86 010 6891 8696.
E-mail address: bitkeningsun@yahoo.com.cn (K. Sun).

0378-7753/$ – see front matter © 2012 Elsevier B.V. All rights reserved.
doi:10.1016/j.jpowsour.2012.03.006

body from the graphite die and lowered the bulk density of the specimen. The maximum bulk density of SPS specimen was approximately 85% of theoretical one [37]. It is not possible to apply SPS in the sintering of thin film electrolyte which is mostly employed in SOFCs.

Recently, a new type of sintering technique named flash sintering was reported by Raj et al. [39]. Flash sintering has been demonstrated in several oxides including cubic yttria doped zirconia (8YSZ and 3YSZ), cobalt manganese oxide (Co_2MnO_4) [39]. It was showed that 3YSZ could be sintered in a few seconds at 850 °C to full density by applying a DC electrical field of 120 V cm^{-1}. Moreover, it was demonstrated that the application of DC electrical field could strongly retard grain growth [40–44].

Due to the relatively higher ionic conductivity of GDC, we suggest that GDC would be sintered at a lower temperature with an applied electrical field. To our current knowledge, no relative research has been done yet.

In this paper, we studied the sinter behavior and grain sizes of GDC specimens under various applied DC electric fields. As reported below, GDC could be sintered to fully dense at 545 °C, much lower than conventional sinter temperature, and several seconds was needed. At the same time, through SEM analysis, we found that grain sizes of GDC were decreasing with the increase of the applied fields.

2. Materials and methods

Commercial $Ce_{0.8}Gd_{0.2}O_{1.9}$ powder (purity >99.84%, with impurities of SiO_2 0.0686%, SO_3 0.0463%, Al_2O_3 0.0380%, particle sizes 0.5–0.3 μm, Ningbo Institute of Materials Technology & Engineering, Chinese Academy of Sciences) used as raw material was mixed with 5-wt% binder (PVA, Sinopharm Chemical Reagent Co., Ltd., China). The mixed powder was pressed into strip shaped specimens with a pressure of 470 MPa. The specimens were then pre-sintered at 800 °C for 4 h. These specimens had a green density of 78.0 ± 1.5%. Two holes with a diameter of 1.0 ± 0.1 cm were drilled on both ends of the specimen in order to connect with platinum wires. The distance between the holes was 20 mm ± 0.5 mm. The specimens were grinded into a dog bone shape with a rectangular cross section of 3.2 mm × 1.24 mm.

Sintering was performed in a dilatometry instrument (DIL 402 PC, Netzsch Corp., Germany) at a heating rate of 10 °C min^{-1} from room temperature to 1600 °C or less. Two platinum electrodes were attached to the drilled holes of the specimens to apply a constant voltage. The applied field was supplied by a common power supply. The current was measured with an amperemeter. Fig. 1 shows the detailed schematic. After the specimen annealing at 900 °C, the *I–E* curve was measured in the 0–60 V cm^{-1} range supplied by a power supply at 900 °C, 800 °C, 700 °C, 600 °C and 500 °C. The current was measured with an amperemeter.

The micrographs of flash sintered specimens were analyzed by scanning electron microscopy (SEM, Quanta FEG 250, FEI). To prepare the SEM sample, a thin layer of Au was coated onto the as flash sintered specimens.

3. Results and discussion

3.1. Flash sintering and conventional sintering (without field)

The function of the shrinkage versus the temperature for different DC applied field values is shown in Fig. 2(a). The true shrinkage strain, given by $\varepsilon = ln(l/l_0)$, where l_0 is the initial gage length and l is the time-dependent gage length as the specimen sintering.

The results in Fig. 2(a) show two different regions of sintering behavior. In the regime of applied field below 15 V cm^{-1},

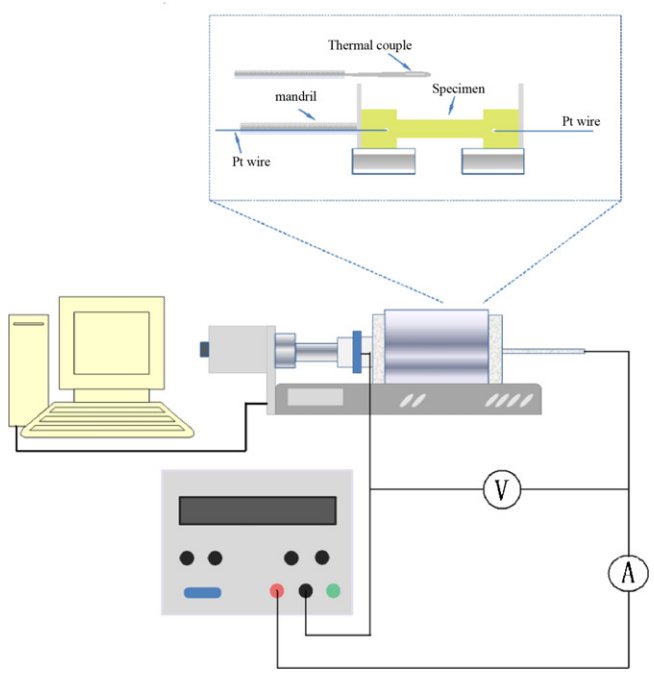

Fig. 1. Schematic of the experimental device. The inset was the specime sketch inside the DIL.

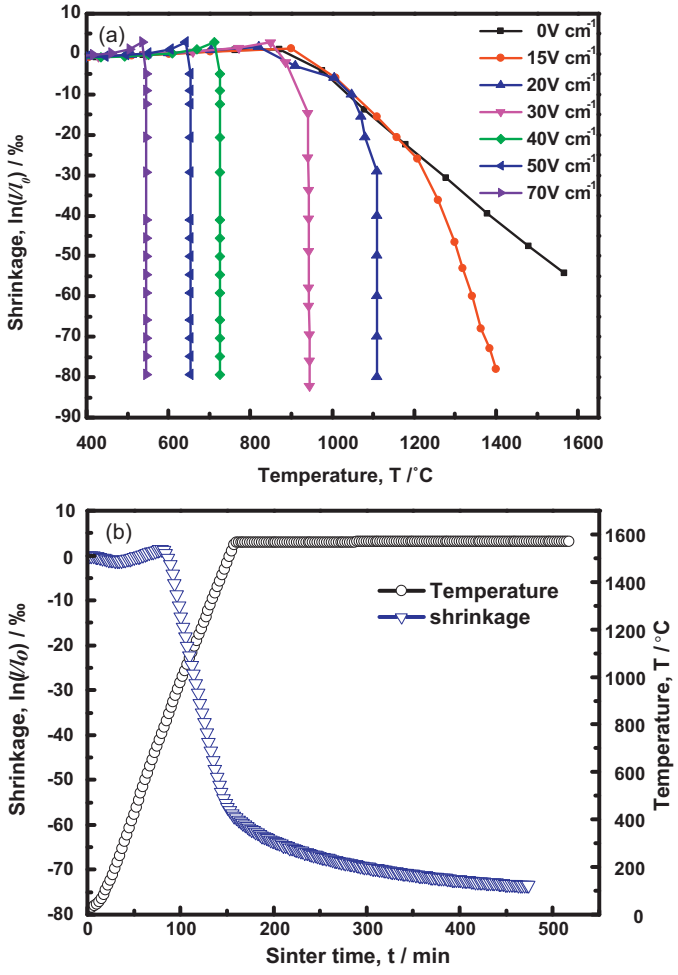

Fig. 2. (a) Linear shrinkage at different applied fields as a function of furnace temperature. All experiments at constant heating rate of 10 °C min^{-1}. (b) Linear shrinkage of conventional sintering as a function of furnace temperature. Heating rate was 10 °C min^{-1}.

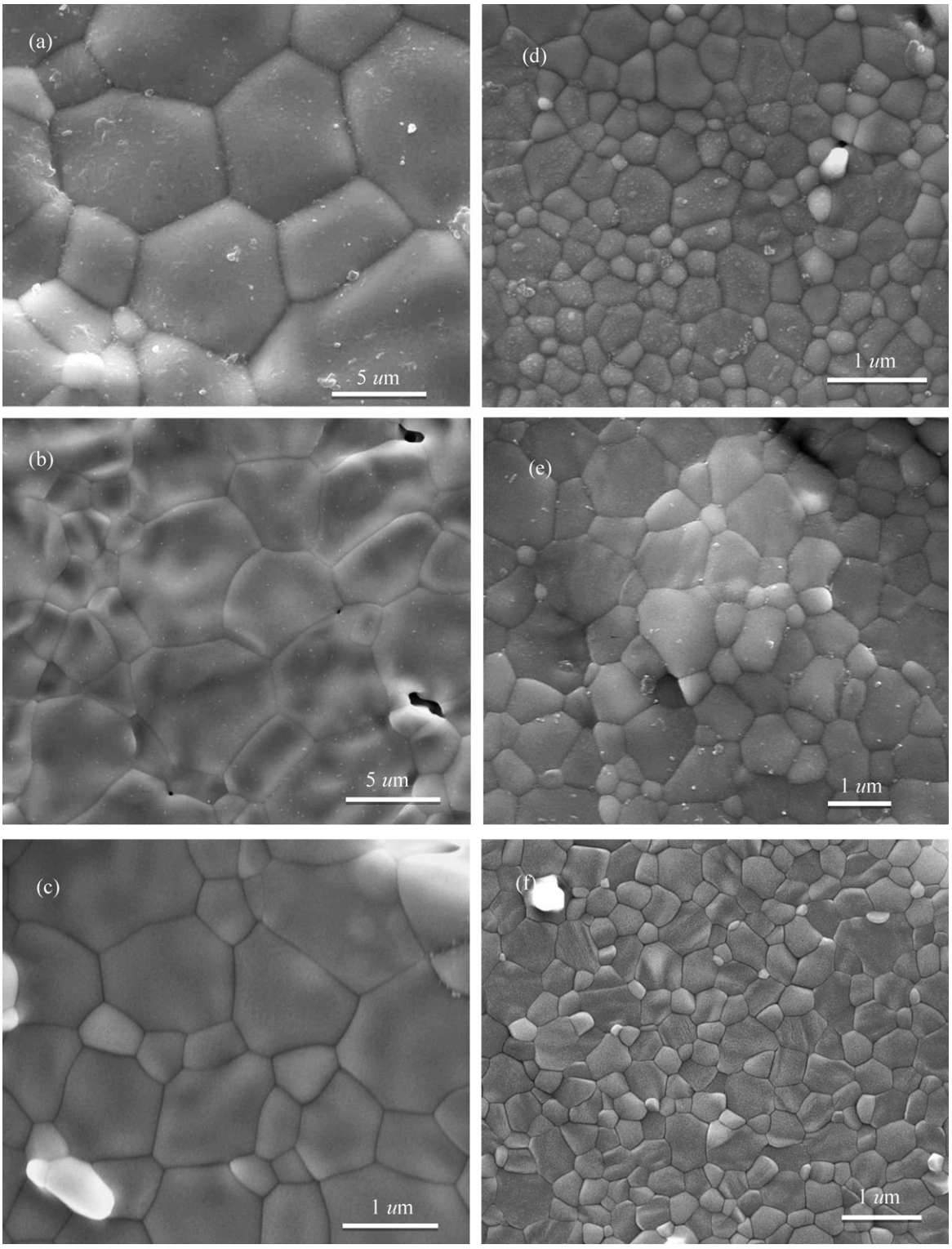

Fig. 3. Scanning electron micrographs of the samples sintered with or without ($0\,V\,cm^{-1}$) the application of electrical field. (a) $0\,V\,cm^{-1}$, (b) $20\,V\,cm^{-1}$, (c) $30\,V\,cm^{-1}$, (d) $40\,V\,cm^{-1}$, (e) $50\,V\,cm^{-1}$ and (f) $70\,V\,cm^{-1}$.

ε gradually increased. This regime was so-called field assisted sintering techniques (FAST) sintering. Above $20\,V\,cm^{-1}$ sintering occurs in only a few seconds called flash sintering. With the increase of the applied field, the temperature of the onset of sintering decreased. Sintering occurs at just about 545 °C, when applied a field of $70\,V\,cm^{-1}$, and 645 °C, 725 °C, 945 °C, 1109 °C for 50, 40, 30, $20\,V\,cm^{-1}$ correspondingly. The final shrinkage reached about −80‰ when the applied field was above $20\,V\,cm^{-1}$.

The shrinkage strain versus temperature data for GDC without applied field (at $0\,V\,cm^{-1}$) is separately given in Fig. 2(b). This is also the conventional sintering approach. The specimen was heated up

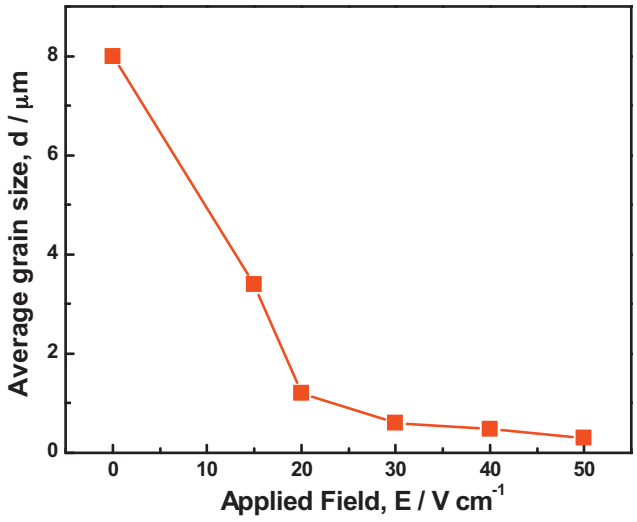

Fig. 4. Grain size as a function of a DC applied electrical field.

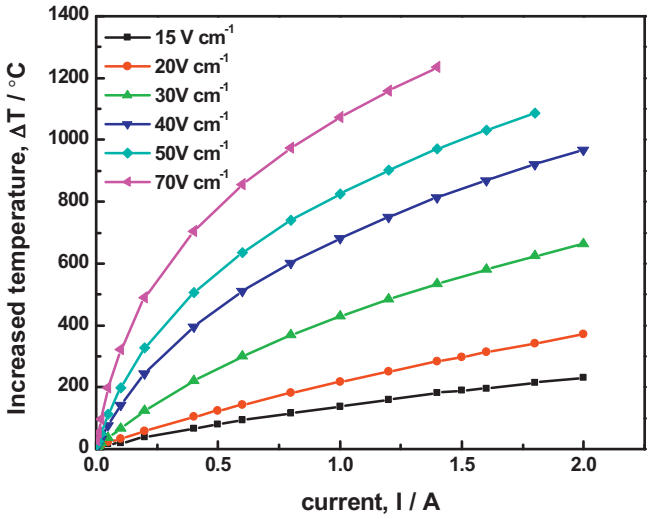

Fig. 5. Calculated temperature rise of specimen caused by Joule heating at different current values at different applied field.

to 1570 °C at a heating rate of 10 °C min^{-1} and then held for 6 h. The final density is reached at a shrinkage strain of −74‰. Compared Fig. 2(a) and (b), it is easy to deduce that the specimens were sintered to fully dense under the application of DC electrical field. This could be further confirmed by SEM analysis.

3.2. SEM micrographs and grain size

The SEM micrographs of the samples sintered at various applied fields were shown in Fig. 3. The samples were as flash sintered specimens with a thin layer of Au. All the samples were sintered to fully dense with only a few close pores (Fig. 3(b)–(d)).

The grain sizes were measured from images taken with Quanta FEG 250 scanning electron microscopy (SEM). The mean grain sizes were determined by linear intercept method. The relationship between applied field and the average grain size was shown in Fig. 4 and Table 1. A reduction in grain growth has been observed in the flash sintering of GDC. The grain size was systematically decreasing with the increased values of applied field, which implies that the grain growth was suppressed by the electrical field. The mechanism for the retardation of grain growth is still unclear, but could be partly explained by two mechanisms: (1) Joule heating at the grain boundaries and (2) reduction in the grain boundary energy γ_{gb} (the driving force) by the interaction of the field with the space charge [42]. In this paper we focus on the influence of Joule heating at the grain boundaries. These details are discussed in Section 3.3.

Notice the average grain sizes of flash-sintered GDC under the applied field of 40 (0.5 μm) and 50 V cm^{-1} (0.3 μm) was very close to the grain size of the commercial raw material (0.5–0.3 μm). It could be supposed that the GDC powder was suddenly sintered to dense without any obvious grain growth. How this happened need to be further studied. Besides, no correlation between the shape of the specimens and the direction of the applied field was found,

Table 1
Average grain sizes of GDC at different flash sintering electrical fields.

Applied field (V cm^{-1})	Flash sintering temperature (°C)	Average grain size (μm)
0	–	8.0
15	–	3.4
20	1109	1.2
30	945	0.6
40	725	0.5
50	654	0.3

implying that the direction of the electrical current did not have an influence on migration of the grain boundaries during sintering.

3.3. Estimate of Joule heating by power dissipation and black body radiation

An approximate estimate of the temperature increase in the specimen can be obtained by assuming that the specimen radiates like a black body, with an emissivity equal to unity (for most oxides this value is ~0.9), and that radiation losses are far greater than convective heat loss to the environment (this is nominally true if the specimen is at dull-red heat when its temperature is ~800 °C). The rise in temperature is then obtained in a straightforward way by equating the black body radiation to the electrical power input.

If the specimen is considered as a uniformly heats up monolithic body, we could use the Stefan Boltzmann law of black body radiation to calculate the temperature increase of the specimen [39,42,43]. The Stefan Boltzmann law was given by $M = \sigma T^4$, where M in units of W m^{-2} is the heat radiated from the body, universal constant σ equal to 5.67×10^{-8} W m^2 K^{-4}, and T (K) is the temperature in Kelvin. The rise in the specimen temperature is estimated by equating the energy expended in the specimen due to the applied DC field, to the energy radiated from the specimen, by using the following equation:

$$M_0 + \frac{\Delta W}{A} = \sigma(T_0 + \Delta T)^4 \quad (1)$$

$$\Delta W = EI \quad (2)$$

where ΔT is the increased temperature of the body due to Joule dissipation of the electrical energy. M_0 is the radiated energy from the specimen at temperature T_0, without the electric field. ΔW is the electrical energy expended in the specimen (in Watts), and A is the total surface area of the specimen. For our experiment the $A = 1.78 \times 10^{-4}$ m^2. The temperature increasing in the specimen is ΔT. T_E is the true temperature of the specimen at applied electrical field. Substituting $M_0 = \sigma T_0^4$, we obtain that:

$$\Delta T = \sqrt[4]{T_0^4 + \frac{\Delta \Omega}{\sigma A}} - T_0 \quad (3)$$

$$T_E = T_0 + \Delta T \quad (4)$$

The calculated results are shown in Fig. 5 and Table 2. From these results, we could easily find that when the flash sintering occurs,

Table 2
Estimated of ΔT and T_E caused by Joule heating at different current values for different applied electric field.

Field (V cm^{-1})	I = 0.5 A			I = 1.0 A			I = 1.5 A			I = 2.0 A		
	T_0 (°C)	T_E (°C)	ΔT (°C)	T_0 (°C)	T_E (°C)	ΔT (°C)	T_0 (°C)	T_E (°C)	ΔT (°C)	T_0 (°C)	T_E (°C)	ΔT (°C)
15	1287	1368	81	1340	1479	139	1370	1559	189	1400	1630	230
20	1190	1284	103	1214	1430	210	1217	1515	298	1218	1588	370
30	957	1217	260	957	1386	429	957	1515	558	957	1621	664
40	730	1187	457	730	1412	682	730	1572	824	730	1699	969
50	660	1239	575	660	1486	826	660	1661	1001	–	–	–
70	545	1331	786	545	1618	1073	–	–	–	–	–	–

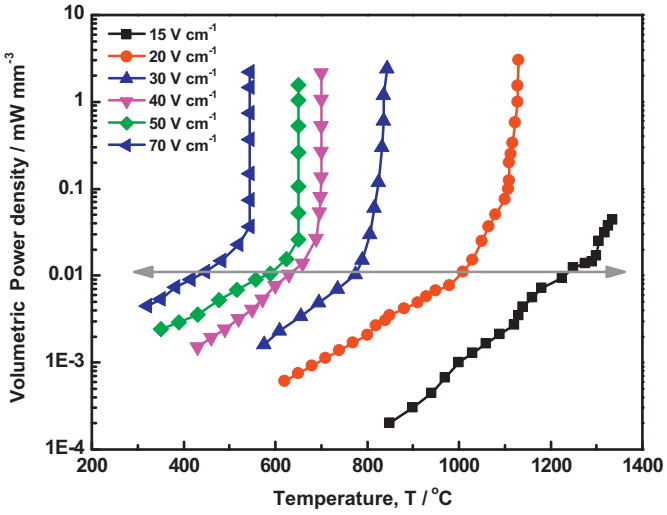

Fig. 6. Power dissipation in the sample as a function of temperature under different applied electrical fields.

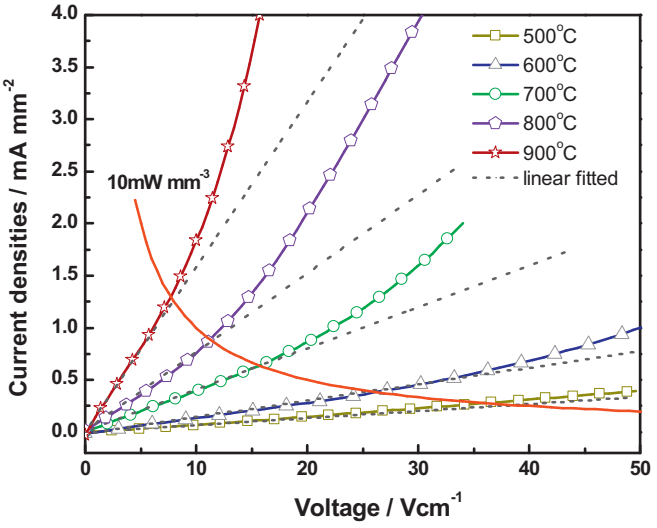

Fig. 7. Current–voltage curve after annealing at 900 °C.

the true temperature of the specimen was as high as 1600 °C (see Table 2), which was large enough to sinter GDC specimen to fully density. This result is readily consistent with the predicted temperature distribution of the zirconia samples under the flash sintering condition through Finite Element Modeling simulations by Grasso [45] and further demonstrates the Joule heating hypothesis.

3.4. Power density dissipation

An Arrhenius plot showing the power dissipation as a function of temperature is shown. The power density was calculated by EI/V, where E is the applied field, I is the current at the applied field and at the respective temperature, V is volume of the specimen. Flash sintering was characterized by the onset of a power-surge, which was not seen in the case of FAST sintering. We note that the onset of flash sintering occurs at a power density level of about 10 mW mm^{-3} (Fig. 6).

Joule heating is defined as an increase in the specimen temperature from the dissipation of electrical energy. Experimentally it can be detected by a divergence of the I–E curve from linear, Ohmic behavior, as the applied voltage is increased, while the furnace temperature is held constant. We determined the significant onset of the Joule heating by measured the I–E curve at 600 °C, 700 °C, 800 °C and 900 °C after the sample was annealed at 900 °C for 4 h. The results are reported in Fig. 7. In each case, the curves begin to deviate from linearity when the power input into the sample was greater than 10 mW. The inference is that above this level of power input Joule heating of the specimen was enough to produce a measurable nonlinearity in the ionic conductivity of the specimen. The turning point of the linear behavior to nonlinear behavior suggested the Joule heating of the sample. From Fig. 7 we deduced the onset of Joule heating was also 10 mW mm^{-3}. Synthesizes the above analysis, we can conclude that the flash sintering is aroused by the Joule heating generated from the applied direct current.

4. Conclusions

We have shown that GDC can be sintered to full dense in just a few seconds at very low temperatures. This process was seen previously in YSZ, and is expected to be for ionic conductors, In addition, it will much more likely to occur if the ion conductivity was higher. As expected, flash sintering was successfully applied in the case of GDC, and the onset value of electrical field is 20 V cm^{-1}, lower than that of YSZ (30 V cm^{-1} for 8YSZ and 60 V cm^{-1} for 3YSZ) [46,47]. The power dissipation is ~10 mW mm^{-3}, which equals that value of the YSZ. SEM analysis showed that with the increase of applied electrical field, the gain sizes of flash sintered GDC were decreasing until the grain size was the same as the raw material. This is believed to be beneficial to the mechanical properties of GDC electrolyte for SOFCs.

With flash sintering, we could use less expensive commercial GDC as raw material without adding any sintering aids to obtain fully dense GDC electrolyte. That will be helpful to lower the material cost as well as keep the ionic conductivity of GDC electrolyte. At the same time, the lower temperature and a short duration of flash sintering will greatly reduce the cost of energy and undesired reactions between GDC and other components. Even more important, the densification of electrolyte finished in very lower temperature could bring a novel way to build the orderly anode nanostructure of SOFCs. This is because the main difficulty currently in building the orderly anode nano- or micro structure is the collapsing caused by the high temperature in electrolyte-anode co-sintering process.

Acknowledgment

This work was supported by the National Natural Science Foundation of China under contract No. 21076023 and No. 21006006.

References

[1] N.Q. Minh, J. Am. Ceram. Soc. 76 (1993) 563–588.
[2] R. Doshi, V.L. Richards, J.D. Carter, X. Wang, M. Krumpelt, J. Electrochem. Soc. 146 (1999) 1273.
[3] E.D. Wachsman, K.T. Lee, Science 334 (2011) 935.
[4] S. Wang, H. Inaba, H. Tagawa, T. Hashimoto, J. Electrochem. Soc. 144 (1997) 4076–4080.
[5] Y.J. Leng, S.H. Chan, S.P. Jiang, K.A. Khor, Solid State Ionics 170 (2004) 9–15.
[6] S.Q. Hui, J. Roller, S. Yick, X.G. Zhang, C.D. Petit, Y. Xie, R. Maric, D. Ghosh, J. Power Sources 172 (2007) 493–502.
[7] B.C.H. Steel, A. Heinzel, Nature 414 (2001) 345–352.
[8] T.H. Etsell, S.N. Flengas, Chem. Rev. 70 (1970) 339.
[9] J.G. Cheng, S.W. Zha, J. Huang, X.Q. Liu, G.Y. Meng, Mater. Chem. Phys. 78 (2003) 791–795.
[10] A. Bieberle-Hütter, D. Beckel, A. Infortuna, U.P. Muecke, J.L.M. Rupp, L.J. Gauckler, S. Rey-Mermet, P. Muralt, N.R. Bieri, N. Hotz, M.J. Stutz, D. Poulikakos, P. Heeb, P. Müller, A. Bernard, R. Gmür, T. Hocker, J. Power Sources 177 (2008) 23–130.
[11] D. Nikbin, Fuel Cell Rev. (April/May) (2006) 21–24.
[12] S.B. Schaevitz, A. Franz, R. Barton, A.P. Ludwiszewski, (2006) US 2006/0263655 A1.
[13] G.J. LaO, H.J. In, E. Crumlin, G. Barbastathis, Y.S. Horn, Int. J. Energy Res. 31 (2007) 548–575.
[14] E. Aneggi, M. Boaro, C. Leitenburg, G. Dolcetti, A. Trovarelli, J. Alloys Compd. 408–412 (2006) 1096–1102.
[15] C. Fu, S.H. Chan, Q. Liu, X. Ge, G. Pasciak, Int. J. Hydrogen Energy 35 (2010) 301–307.
[16] R.K. Lenka, T. Mahata, P.K. Sinha, B.P. Sharma, J. Am. Ceram. Soc. 89 (12) (2006) 3871–3873.
[17] K.R. Reddy, K. Karan, J. Electroceram. 15 (2005) 45–56.
[18] M. Morales, J.J. Roa, X.G. Capdevila, M. Segarra, S. Piñolb, Acta Mater. 58 (2010) 2504–2509.
[19] R.A. Tsoga, A. Naoumidis, D. Stover, Solid State Ionics 135 (2000) p.403.
[20] A. Moure, J. Tartaj, C. Moure, J. Am. Ceram. Soc. 92 (2009) 2197–2203.
[21] C. Kleinlogel, L.J. Gauckler, Solid State Ionics 135 (2000) 567–573.
[22] P.L. Chen, I.W. Chen, J. Am. Ceram. Soc. 76 (1993) 1577–1583.
[23] Q.L. Liu, S.H. Chan, C.J. Fu, G. Pasciak, Electrochem. Commun. 11 (2009) 871–874.
[24] Y.B. Go, A.J. Jacobson, Chem. Mater. 19 (2007) 4702–4709.
[25] T. Mori, R. Buchanan, D.R. Ou, F. Ye, T. Kobayashi, J.D. Kim, J. Zou, J. Drennan, J. Solid State Electrochem. 12 (2008) 841–849.
[26] V. Gil, J. Tartaj, C. Moure, P. Duran, Ceramics International 33 (2007) 471–475.
[27] T.S. Zhang, J. Ma, Y.J. Leng, J.A. Kilner, J. Cryst. Growth 274 (2005) 603–611.
[28] D.P. Fagg, J.C.C. Abrantes, D.P. Coll, P. Nunez, V.V. Kharton, J.R. Frade, Electrochim. Acta 48 (2003) 1023–1029.
[29] S.H. Park, H.I. Yoo, Solid State Ionics 176 (2005) 1485–1490.
[30] C.M. Kleinlogel, Ph.D thesis. Swiss Federal Institute of Technology, Zurich, 1999.
[31] C. Kleinlogel, L.J. Gauckler, Solid State Ionics 135 (2000) 567.
[32] C. Kleinlogel, L.J. Gauckler, Adv. Mater. 13 (2001) 1081.
[33] J.R. Groza, S.H. Risbud, K. Yamazaki, J. Mater. Res. 7 (1992) p.2643.
[34] R.S. Mishra, S.H. Risbud, A.K. Mukherjee, J. Mater. Res. 13 (1998) p.86.
[35] L. Gao, J.S. Hong, H. Miyamoto, S.D. De La Torre, J. Inorg. Mater. 13 (1) (1998) 18–22.
[36] U.A. Tamburini, J.E. Garay, Z.A. Munir, Fast low-temperature consolidation of bulk nanometric ceramic materials, Scr. Mater. 54 (5) (2006) 823–828.
[37] T. Mori, T. Kobayashi, Y. Wang, J. Drennan, T. Nishimura, J.G. Li, H. Kobayashi, J. Am. Ceram. Soc. 88 (7) (2005) 1981–1984.
[38] U.A. Tamburini, F. Maglia, G. Chiodelli, A. Tacca, G. Spinolo, P. Riello, S. Bucella, Z.A. Munir, Adv. Funct. Mater. 16 (18) (2006) 2363-2368.
[39] A.L.G. Prette, M. Cologna, V. Sglavo, R. Raj, J. Power Sources 196 (2011) 2061–2065.
[40] M. Cologna, B. Rashkova, R. Raj, J. Am. Ceram. Soc. 93 (2010) 3556–3559.
[41] S. Ghosh, A.H. Chokshi, P. Lee, R. Raj, J. Am. Ceram. Soc. 92 (2009) 185.
[42] H. Conrad, J. Am. Ceram. Soc. 94 (2011) 3641–3642.
[43] R. Raj, M. Cologna, S. John, C. Francis, J. Am. Ceram. Soc. 94 (7) (2011) 1941–1965.
[44] D. Yang, R. Raj, H. Conrad, J. Am. Ceram. Soc. 93 (2010) 2935–2937.
[45] S. Grasso, Y. Sakka, N. Rendorff, C.F. Hu, G. Maizza, H. Borodianska, O. Vasylkiv, J. Ceram. Soc. Jpn. 119 (2) (2011) 144–146.
[46] M. Cologna, A.L.G. Prette, R. Raj, J. Am. Ceram. Soc. 94 (2011) 316–319.
[47] M. Cologna, R. Raj, J. Am. Ceram. Soc. 94 (2011) 391–395.